The dynamics of a viscous soap film with soluble surfactant

Jean-Marc Chomaz

J. Fluid Mech. (2001), *vol.* 442, *pp.* 387–409. Printed in the United Kingdom

The dynamics of a viscous soap film with soluble surfactant

By JEAN-MARC CHOMAZ

LadHyX, CNRS–Ecole Polytechnique, 91128 Palaiseau, France

(Received 25 October 1999 and in revised form 24 March 2001)

Nearly two decades ago, Couder (1981) and Gharib & Derango (1989) used soap films to perform classical hydrodynamics experiments on two-dimensional flows. Recently soap films have received renewed interest and experimental investigations published in the past few years call for a proper analysis of soap film dynamics. In the present paper, we derive the leading-order approximation for the dynamics of a flat soap film under the sole assumption that the typical length scale of the flow parallel to the film surface is large compared to the film thickness. The evolution equations governing the leading-order film thickness, two-dimensional velocities (locally averaged across the film thickness), average surfactant concentration in the interstitial liquid, and surface surfactant concentration are given and compared to similar results from the literature. Then we show that a sufficient condition for the film velocity distribution to comply with the Navier–Stokes equations is that the typical flow velocity be small compared to the Marangoni elastic wave velocity. In that case the thickness variations are slaved to the velocity field in a very specific way that seems consistent with recent experimental observations. When fluid velocities are of the order of the elastic wave speed, we show that the dynamics are generally very specific to a soap film except if the fluid viscosity and the surfactant solubility are neglected. In that case, the compressible Euler equations are recovered and the soap film behaves like a two-dimensional gas with an unusual ratio of specific heat capacities equal to unity.

1. Introduction

Water films have been studied since the pioneering papers of Savart (1833*a*, *b*), Boys (1890), and, later, of Squire (1953) and Taylor (1959) because of their natural beauty, their theoretical interest, and the variety of applications ranging from atomization and sprays in combustion to curtain coating processes. Water films sustain waves originating from the interactions between the capillary waves which develop on their interfaces.

When soap is added to water, the dependence of surface tension on the superficial soap concentration makes the film elastic and therefore reduces its tendency to break. In this case, the soap film may sustain large-scale in-plane motions. This property has allowed soap films to be used as a convenient two-dimensional fluid. In Couder's (1981) experiments a membrane, stretched on a large frame, was used as a two-dimensional towing tank. Further investigations were reported by Gharib & Derango (1989) who designed a soap tunnel by pulling a horizontal membrane downstream of the test section with a clear water jet. Recently, a new way to produce a soap tunnel has been proposed and tested by Kellay, Wu & Goldburg (1995). In their experiment a vertical membrane is continuously stretched between two wires

emerging from a reservoir from which soap solution is *twinkling* down. These soap film experiments have attracted the curiosity of numerous scientists who have performed modern, careful, and precise mesurements of various two-dimensional flows such as, in particular, Wu *et al.* (1995), Kellay *et al.* (1995, 1998), Rutgers, Wu & Bhagavatula (1996), Goldburg, Rutgers & Wu (1997), Afenchenko *et al.* (1998), Martin *et al.* (1998), Rivera, Vorobieff & Ecke (1998), Vega, Higuera & Wiedman (1998), Vorobieff, Rivera & Ecke (1999), Boudaoud, Couder & Ben Amar (1999), Burgess *et al.* (1999), Horváth *et al.* (2000), Rivera & Wu (2000).

Despite this continuous interest, a fundamental question remains unanswered: whether soap films obey the classical two-dimensional Navier–Stokes equations and, for example, demonstrate the existence of the inverse cascade in two-dimensional turbulence, or soap films suffer specific dynamics that make them useless for the investigation of fundamental problems of two-dimensional hydrodynamics? On the solution of this dilemma depends the pertinence of soap film experiments. On the basis of appropriate physical considerations, Couder, Chomaz & Rabaud (1989) (and later on Chomaz & Cathalau 1990, and Chomaz & Costa 1998) have shown that a two-dimensional description may be achieved if the velocity is small compared to the elastic wave velocity. But as yet, no proper demonstrations have validated their assumptions; furthermore no results at all are at present available for when the soap film velocity is close to the elastic wave velocity.

In § 3 of the present contribution a complete analysis of the three-dimensional soap film dynamics is presented using the asymptotic lubrication theory which assumes only that the thickness of the film is small compared to the characteristic length scale of the in-plane flow. The analysis gives both the physics of the equilibrium at play in the free film and the order of magnitude of the neglected effects. The paper will make systematic use of the notations and results of recent contributions by Edwards & Oron (1995) and Oron, Davis & Bankoff (1997) to which the reader should refer. The mathematical analysis of thin film dynamics using asymptotic expansions, multiple scale analysis, the long wave assumption or equivalently the homogenization technique is standard and applications to free films and films coating a solid surface have been reviewed in Oron *et al.* (1997) and Ida & Miksis (1998*a*). Only a few particular contributions are mentioned here. Evolution equations for the surfactant have been derived in Waxman (1984) and Stone (1990). The nonlinear dynamics of two-dimensional free films may be found in Prévost & Gallez (1986) and in Erneux & Davis (1993) for the case without surfactant, and in Sharma & Ruckenstein (1986) and De Wit, Gallez & Christov (1994) for the case with insoluble surfactant. The three-dimensional dynamics of an arbitrary film have been analysed by van de Fliert, Howell & Ockendon (1995) and extended by Ida & Miksis (1998*a*) to take surfactant effects into account. Section 3 of the present contribution may be viewed as an application to a planar geometry of the general description given by Ida & Miksis (1998*b*). It extends the latter study by including surfactant solubility and deriving the associated evolution equation for the averaged surfactant concentration in the interstitial liquid.

Although the present derivation of § 3 shares results with De Wit *et al.* (1994) and Ida & Miksis (1998*a*, *b*) it differs from them by the scaling assumption: previous studies concentrate on the motion induced by surfaces or van der Waals forces whereas, here, we consider the fate of pre-existing motion. As a result, the order of magnitude of the planar velocity is treated as a free parameter instead of being fixed by viscous effects. This leads to new scalings for the velocity, the pressure, the thickness variation, and the time scales and imposes the introduction of new non-dimensional

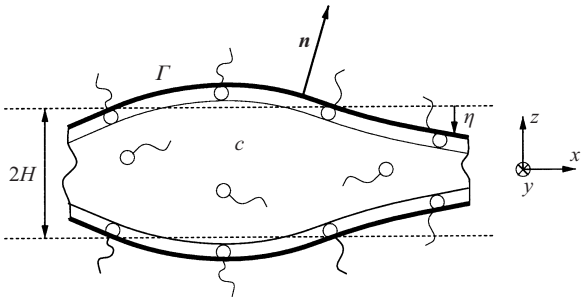

FIGURE 1. Soap film internal structure.

parameters. The leading-order equations so obtained are specific to soap films and their relations to the Navier–Stokes equations are discussed in § 4. We make use of the flexibility brought by the new scaling assumptions and consider different limit cases, only one of which results in incompressible two-dimensional Navier–Stokes dynamics and another in the compressible Euler equations for a two-dimensional gas with an unusual ratio of specific heats $\gamma = 1$. In no cases will a soap film satisfy the compressible two-dimensional Navier–Stokes equations. The importance of the ratio between the typical planar velocity and the elastic Marangoni wave velocity is rigorously established.

2. Soap film equations

As described in Couder *et al.* (1989), soap films used in hydrodynamics experiments may be seen as a three-layer structure: two surfaces and a bulk fluid in-between (figure 1). For simplicity, a single species of surfactant will be considered, this surfactant (from now on called the soap) being allowed to migrate between the three phases (soluble surfactant). The film is considered flat as is indeed the case in vertical soap film experiments or when the bending of the soap film under its weight is compensated by a pressure difference between the two surfaces (see Couder *et al.* 1989 for details). Only symmetric perturbations will be considered and, therefore, each surface phase will be a mirror of the other. The surface concentration of soap will be denoted by Γ whereas c will designate the interstitial soap concentration.

The bulk fluid moves with a three-dimensional velocity $\boldsymbol{u} = (u, v, w)$. The fluid is assumed incompressible with a density ρ and a kinematic viscosity $\nu = \mu/\rho$ independent of the amount of soap. The pressure inside the film is denoted p. The two surface phases are symmetrically deformed and located at the elevation $z = \pm\eta(x, y, t)$, the film being assumed flat on average in the plane (x, y). A surface tension σ applies to each surface.

The bulk fluid flow is governed by the incompressible Navier–Stokes equation and the bulk soap concentration by the advection diffusion equation:

$$\left.\begin{aligned} \nabla^* \cdot \boldsymbol{u} &= 0, \\ \frac{\partial \boldsymbol{u}}{\partial t} + \boldsymbol{u} \cdot \nabla^* \boldsymbol{u} &= -\frac{1}{\rho}\nabla^* p + \nu \nabla^{*2} \boldsymbol{u}, \\ \frac{\partial c}{\partial t} + \boldsymbol{u} \cdot \nabla^* c &= D \nabla^{*2} c, \end{aligned}\right\} \tag{2.1}$$

where D is the soap diffusivity in the bulk fluid and ∇^* stands for the three-dimensional nabla operator in order to differentiate it from its two-dimensional counterpart (in the x, y-plane) denoted ∇.

Although potential volume forces, like gravity or van der Waals forces, may be taken into account by adding a $\nabla^*\phi$ term on the right-hand side of the momentum equation (2.1) (see Edwards & Oron 1995; Ida & Miksis 1995, 1998*a*; and Oron *et al.* 1997 for details), they will be ignored as a first step. This assumption is realistic, since soap films used in experiments are a few microns thick, so that direct interactions between surfaces (van der Waals forces possibly represented by a disjoining pressure) are negligible.

This system of bulk fluid equations is completed by boundary conditions at both free surfaces and because of the assumed symmetry only the conditions at the upper surface will be explicitly given. The kinematic condition, at the interface $z = \eta(x, y, t)$, reads

$$\frac{\partial \eta}{\partial t} + \boldsymbol{u} \cdot \nabla^* \eta = w, \tag{2.2}$$

whereas the force balance at each interface may be written

$$(p - p_a + 2\mathscr{C}\sigma)\boldsymbol{n} = \nabla_{\mathbf{s}}\sigma + \mu(\nabla^*\boldsymbol{u} + \nabla^*\boldsymbol{u}^t) \cdot \boldsymbol{n}, \tag{2.3}$$

following Levich & Krylov (1969) and using the notation of Edwards & Oron (1995). The pressure in the air surrounding the film is denoted by p_a, the unit vector normal to the upper surface and oriented toward the air by $\boldsymbol{n}$ with

$$\boldsymbol{n} = \left(-\frac{\partial \eta}{\partial x}, -\frac{\partial \eta}{\partial y}, 1\right)\left(1 + \left(\frac{\partial \eta}{\partial x}\right)^2 + \left(\frac{\partial \eta}{\partial y}\right)^2\right)^{-1/2}, \tag{2.4}$$

$2\mathscr{C}$ is the mean surface curvature (defined by $2\mathscr{C} = -\nabla^* \cdot \boldsymbol{n}$)

$$2\mathscr{C} = \frac{\dfrac{\partial^2 \eta}{\partial x^2}\left(1 + \left(\dfrac{\partial \eta}{\partial y}\right)^2\right) - 2\dfrac{\partial \eta}{\partial x}\dfrac{\partial \eta}{\partial y}\dfrac{\partial^2 \eta}{\partial x \partial y} + \dfrac{\partial^2 \eta}{\partial y^2}\left(1 + \left(\dfrac{\partial \eta}{\partial x}\right)^2\right)}{\left(1 + \left(\dfrac{\partial \eta}{\partial x}\right)^2 + \left(\dfrac{\partial \eta}{\partial y}\right)^2\right)^{3/2}}, \tag{2.5}$$

$\nabla_{\mathbf{s}}$ the surface gradient operator

$$\nabla_{\mathbf{s}} = \boldsymbol{I}_{\mathbf{s}} \cdot \nabla^*, \tag{2.6}$$

with $\boldsymbol{I}_{\mathbf{s}}$ the surface idemfactor

$$\boldsymbol{I}_{\mathbf{s}} = \boldsymbol{I} - \boldsymbol{nn} \ (\boldsymbol{I} \text{ the spatial idemfactor}). \tag{2.7}$$

The left-hand side of equation (2.3) corresponds simply to the Young–Laplace law which states that surface tension induces a jump in pressure when the interface is curved. Equation (2.3) projected on the normal $\boldsymbol{n}$ gives

$$p - p_a + 2\mathscr{C}\sigma = \boldsymbol{n} \cdot \mu(\nabla^*\boldsymbol{u} + \nabla^*\boldsymbol{u}^t) \cdot \boldsymbol{n}. \tag{2.8}$$

The right-hand side of equation (2.3) expresses the balance at the interface between the surface tension gradient and the tangential shear stress in the bulk fluid $\mu(\nabla^*\boldsymbol{u} + \nabla^*\boldsymbol{u}^t) \cdot \boldsymbol{n}$. Projected on the two tangents to the interface (not normalized) $\boldsymbol{t}_1 = (1, 0, \partial\eta/\partial x)$ and $\boldsymbol{t}_2 = (0, 1, \partial\eta/\partial y)$ equation (2.3) gives

$$0 = \nabla_{\mathbf{s}}\sigma \cdot \boldsymbol{t}_i + \boldsymbol{t}_i \cdot \mu(\nabla^*\boldsymbol{u} + \nabla^*\boldsymbol{u}^t) \cdot \boldsymbol{n}. \tag{2.9}$$

Terms, like for example $\mu_s \nabla_s^2 \boldsymbol{u}$, may also be added to equation (2.3) to express dissipation in the surface layer due to surface shear viscosity μ_s generated by the adsorbed surfactant. In the present study, such terms will not be considered, although their introduction is straightforward, because the dissipation in the bulk fluid is assumed to dominate for such a thick film.

Except when soap films are flowing into vacuum, air friction should also enter equation (2.3) through an extra term $-\mu_a(\nabla^* \boldsymbol{u}_a + \nabla^* \boldsymbol{u}_a{}^t) \cdot \boldsymbol{n}$ on the right-hand side, where $\boldsymbol{u}_a$ and $-\mu_a$ are the air velocity and viscosity. This effect has been discussed in Couder *et al.* (1989), and although it has been shown to be important (see in particular Rivera & Wu 2000), it is not included here to ease the derivation. Further comments are made later on. Furthermore evaporation of water, essential for thinner films, might be also considered as discussed in Oron *et al.* (1997).

The present paper will concentrate on the leading-order equation governing the evolution of large-scale motions imposed by moving boundaries normal to the film surface (as moving disks or cylinders). The precise details of the interaction with the boundary that involves a meniscus (see Couder *et al.* 1989) will not be described. We will simply consider the initial-value problem without lateral (normal to the film surface) boundaries where a large-scale flow (generally non-potential) is initially imposed arbitrarily. Experimentally the generation of vorticity by laterally moving walls could be avoided by using an electromagnetic field to generate a body force in the plane of the film. This technique was very efficient in generating two-dimensional turbulence in thin stratified extended layers by Paret & Tabeling (1997). It has been very recently implemented with soap films by Riviera & Wu (2000) who have experimentally demonstrated the validity of the two-dimensional Navier–Stokes approximation for soap film dynamics. Another technique to generate initial motion in the film without a wall in conttact with the soap film uses air friction and has been successfully applied by Burgess *et al.* (1999) to study the stability of Kolmogorov flow.

To solve the last equation of the system (2.1), we need a condition on the bulk soap concentration c at the boundary. Following Levich & Krylov (1969), let us call the flux of soap from the bulk film to the surface j, then

$$\left.\begin{aligned} D\boldsymbol{n} \cdot \nabla^* c &= -j, \\ \frac{\partial \Gamma}{\partial t} + \nabla_s \cdot (\boldsymbol{u}\Gamma) &= D_s \nabla_s^2 \Gamma + j, \end{aligned}\right\} \tag{2.10}$$

where D_s is the surface diffusivity of a soap molecule that will be neglected (as we did for the surface viscosity) since the typical length scale of the in-plane motion is considered to be large compared to the thickness of the film. We shall assume that the flux j is dictated by an adsorption–desorption process given by a first-order kinetics:

$$j = (Kc - \Gamma)/\tau, \tag{2.11}$$

where τ is the adsorption–desorption time and Kc is the instantaneous equilibrium surface density, K being a coefficient with the dimension of a length that may be interpreted as the virtual thickness of the interface in terms of soap molecule adsorption. Since soap molecules, composed of a hydrophilic polar head associated with an hydrophobic carbon tail, tend to settle at the surface, K is large (of the order of 4 μm for sodium dodecyl sulfate (SDS) following Rusanov & Krotov 1979) and τ may be large too (from an order of 10^{-2} s for a pure single surfactant agent to an order of 1 s or more when impurities or different surfactants are present;

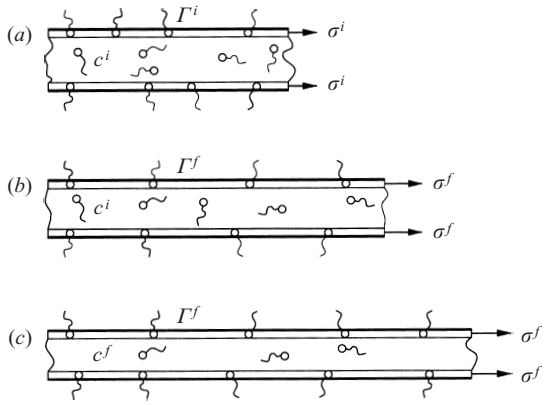

FIGURE 2. Evolution of a membrane under an increase of the applied tension: (*a*) initial state, (*b*) instantaneous response (Marangoni elasticity), (*c*) long-time response (Gibbs elasticity).

see Rusanov & Krotov 1979 for details). These observations are in agreement with the assumption made by many authors, e.g. De Wit *et al.* (1994) or Ida & Miksis (1998*a*, *b*) when modelling thin breaking films, that the soap is insoluble. However, in many two-dimensional dynamics experiments, the characteristic hydrodynamic time scale is about 1 s and the mean thickness is about K so that the soap molecule flux between surfaces and bulk fluid cannot be neglected. The present analysis will retain this adsorption–desorption effect and therefore extend the Ida & Miksis (1998*b*) analysis.

To close the system of equations, we need to describe the evolution of the surface tension σ that enters the problem through the surface stress balance (2.3). The simplest equation of state for the surface tension reads

$$\sigma = \sigma_a - \sigma_r \Gamma, \tag{2.12}$$

where σ_a is the surface tension in the absence of surfactant and σ_r accounts for the elasticity of the film. More generally, since $\sigma_r \Gamma$ may not be small compared to σ_a, equation (2.12) may be viewed as a linearized expression, σ_r being then the elasticity for the typical working concentration of the surfactant. This elasticity is by far the more crucial effect for a soap film to behave as a two-dimensional fluid for which the surface tension replaces the usual pressure. Figure 2 schematically illustrates the stretching of a soap film initially at equilibrium, when suddenly the tension applied to the film is increased from σ^i to σ^f. This evolution subtly involves the elasticity of the film and the adsorption–desorption process. For times shorter than τ (figure 2*b*), the flux of molecules from the bulk fluid to the surface is negligible. The surface of the film therefore increases and, as a result, the surface soap concentration Γ decreases from its initial value Γ^i (given by $\sigma^i = \sigma_a - \sigma_r \Gamma^i$) until it reaches the final value Γ^f (given by $\sigma^f = \sigma_a - \sigma_r \Gamma^f$). At these early times, the initial chemical equilibrium given $Kc^i - \Gamma^i = 0$ is broken and soap molecules start to migrate from the bulk to the surface. In this migration process, the film elongates slowly since j is positive and Γ is fixed at the value Γ^f by the imposed constant tension applied to the film. For times larger than τ (figure 2*c*), j goes back to zero and the new chemical equilibrium given by $Kc^f - \Gamma^f = 0$ is reached. The fast time response of the film is called the Marangoni elasticity and the long time response the Gibbs elasticity.

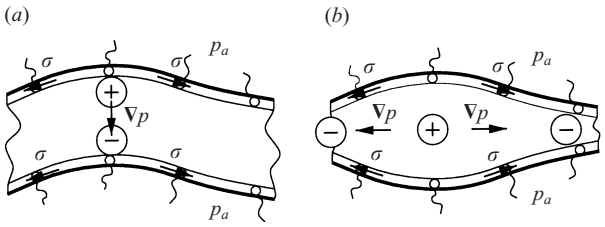

FIGURE 3. Pressure gradient in the case of (*a*) antisymmetric mode (bending mode) and (*b*) symmetric mode.

3. Non-dimensional problem and asymptotic expansion

Before presenting the asymptotic expansion of the problem, it is worth pointing out that the soap film hydrodynamics considered here involve in-plane motion with a large length scale L compared to the mean film thickness $2H$. Therefore, we anticipate that the pressure will be everywhere constrained by the Young–Laplace law, varying as $\sigma_a 2\mathscr{C}$, the mean curvature $\mathscr{C}$ being at most of order H/L^2. At leading order, the pressure gradient will play no role and only viscous forces will be able to balance the surface tension gradient (describing the elasticity of the membrane) in the surface stress equation (2.3). In turn, viscous terms due to velocity shear in the z-direction will dominate in the Navier–Stokes equation (2.1) and transfer the surface force (due to the elasticity) to the bulk fluid. As already pointed out by Taylor (1959) the balances at work in free films radically differ from those in thin films on a solid surface. In the latter case, the pressure is given by the hydrostatic balance at leading order and is compensated by viscous stresses with inertia terms being important at the next order. Therefore, the non-dimensionalization will differ from that of Edwards & Oron (1995).

In Ida & Miksis (1998*a*) the film is not flat. Curvature is then of order L^{-1}, the pressure gradient is dominant and it is balanced by the inertia normal to the centre-surface (see figure 3 and the discussion of § 3.2). This effect deforms the centre-surface as if it were an elastic membrane. At next order the balance described above is recovered.

3.1. *Non-dimensional problem*

The indirect balance between surface forces and bulk film inertia, anticipated above, has already been described in Couder *et al.* (1989) and analysed in De Wit *et al.* (1994) and Ida & Miksis (1998*a*, *b*) (referred to herein as DWGC & IM) for the breaking of a film initially at rest. We shall extend their analysis to the situation where the velocity in the plane of the film is arbitrarily prescribed initially. The typical velocity in the present analysis is a free parameter (whereas in DWGC & IM it is imposed by the surface interaction and viscosity). Therefore, the non-dimensionalization will differ from DWGC & IM to allow more flexibility. Furthermore, we shall consider soluble surfactants and this will add a new degree of freedom in the asymptotic leading-order equations. The basic structure of the flow will turn out to be the one described physically by Couder *et al.* (1989), i.e. a leading-order flow, uniform over the depth of the film, coupled to a Poiseuille secondary flow that uniformly transfers the surface elasticity forces to the bulk fluid. The following asymptotic expansion inspired by DWGC & IM will rigorously establish this particular interplay between surface and bulk forces and between primary and secondary flows. The full derivation

is still given since it throws light on the origin of each term of the leading-order equation and is therefore necessary to understand the physical mechanism at play in the various dominant balances considered in § 4. For the first time, the governing equations for mean velocities, the bulk and surface surfactant concentrations, and film thickness are given for three-dimensional motion of a free film with soluble surfactant.

Let $\epsilon = H/L$ be the expansion parameter and anticipating the dominant balance principle we non-dimensionalize the variables as

$$\left.\begin{gathered} x = x'L, \quad y = y'L, \quad z = z'H = \epsilon z'L, \\ u = u'U, \quad v = v'U, \quad w = \epsilon w'U, \\ t = t'L/U, \quad p = p_a + p'\epsilon\sigma_m/L, \quad \sigma = \sigma_m + \sigma'\rho H U^2 = \sigma_m + \epsilon\sigma'\rho L U^2, \\ \eta = (1+\eta')H, \quad \Gamma = \Gamma'\Gamma_m, \quad c = c'c_m, \end{gathered}\right\} \tag{3.1}$$

where U is the characteristic velocity, Γ_m and c_m are, respectively, the surface and bulk mean concentrations of soap defined by $\Gamma_m = Kc_m$ such that $C_m \equiv \Gamma_m/H + c_m = c_m(1 + K/H)$ is the typical total soap concentration of the solution from which the membrane has been made. The mean surface tension of the film is $\sigma_m = \sigma_a - \sigma_r\Gamma_m$. The pressure variations have been scaled by $\epsilon\sigma_m/L$ anticipating a dominant balance due to the Young–Laplace law. Then, the non-dimensional bulk equations reduce to, dropping the primes of all non-dimensionalized quantities for convenience,

$$\left.\begin{gathered} \frac{\partial u}{\partial x} + \frac{\partial v}{\partial y} + \frac{\partial w}{\partial z} = 0, \\ \frac{\partial u}{\partial t} + u\frac{\partial u}{\partial x} + v\frac{\partial u}{\partial y} + w\frac{\partial u}{\partial z} = -M^{-2}\frac{\partial p}{\partial x} + R^{-1}\left(\frac{\partial^2 u}{\partial x^2} + \frac{\partial^2 u}{\partial y^2} + \epsilon^{-2}\frac{\partial^2 u}{\partial z^2}\right), \\ \frac{\partial v}{\partial t} + u\frac{\partial v}{\partial x} + v\frac{\partial v}{\partial y} + w\frac{\partial v}{\partial z} = -M^{-2}\frac{\partial p}{\partial y} + R^{-1}\left(\frac{\partial^2 v}{\partial x^2} + \frac{\partial^2 v}{\partial y^2} + \epsilon^{-2}\frac{\partial^2 v}{\partial z^2}\right), \\ \frac{\partial w}{\partial t} + u\frac{\partial w}{\partial x} + v\frac{\partial w}{\partial y} + w\frac{\partial w}{\partial z} = -\epsilon^{-2}M^{-2}\frac{\partial p}{\partial z} + R^{-1}\left(\frac{\partial^2 w}{\partial x^2} + \frac{\partial^2 w}{\partial y^2} + \epsilon^{-2}\frac{\partial^2 w}{\partial z^2}\right), \\ \frac{\partial c}{\partial t} + u\frac{\partial c}{\partial x} + v\frac{\partial c}{\partial y} + w\frac{\partial c}{\partial z} = Sc^{-1}R^{-1}\left(\frac{\partial^2 c}{\partial x^2} + \frac{\partial^2 c}{\partial y^2} + \epsilon^{-2}\frac{\partial^2 c}{\partial z^2}\right), \end{gathered}\right\} \tag{3.2}$$

where $M = M_b\epsilon^{-1}$, with $M_b = U/v_b$ the bending Mach number since it compares the bending mode speed $v_b = \sqrt{\sigma_m/H\rho}$ (the bending mode is the antisymmetric mode of the membrane motion due to the tension of the film and for which the elasticity plays no role, see figure 3*a*) to the flow velocity U, and $R = UL/\nu$ is the Reynolds number. The Schmidt number of the soap is $Sc = \nu/D$.

This set of equations is closed by boundary conditions at $z = 1 + \eta$ (the conditions at $z = -1 - \eta$ are symmetric). The non-dimensional equations (2.2), (2.8), (2.9), (2.10), (2.11), (2.12) read at the lowest order in ϵ required to carried on the present asymptotic analysis (see Edwards & Oron 1995 for a systematic expansion of

all the relevant quantities)

$$\left.\begin{aligned}
\frac{\partial \eta}{\partial t}+u\frac{\partial \eta}{\partial x}+v\frac{\partial \eta}{\partial y}&=w,\\
p+2\mathscr{C}(1+\epsilon^2M^2\sigma)&=2M^2R^{-1}\left(\frac{\partial w}{\partial z}-\frac{\partial \eta}{\partial x}\frac{\partial u}{\partial z}-\frac{\partial \eta}{\partial y}\frac{\partial v}{\partial z}+O(\epsilon^2)\right),\\
2\mathscr{C}&=\frac{\partial^2\eta}{\partial x^2}+\frac{\partial^2\eta}{\partial y^2}+O(\epsilon^2),\\
\frac{\partial \sigma}{\partial x}&=\epsilon^{-2}R^{-1}\left(\frac{\partial u}{\partial z}+\epsilon^2\left(-2\frac{\partial \eta}{\partial x}\frac{\partial u}{\partial x}-\frac{\partial \eta}{\partial y}\left(\frac{\partial u}{\partial y}+\frac{\partial v}{\partial x}\right)+\frac{\partial w}{\partial x}\right.\right.\\
&\quad\left.\left.-\frac{\partial \eta}{\partial x}^2\frac{\partial u}{\partial z}-\frac{\partial \eta}{\partial x}\frac{\partial \eta}{\partial y}\frac{\partial v}{\partial z}+2\frac{\partial \eta}{\partial x}\frac{\partial w}{\partial z}\right)+O(\epsilon^4)\right),\\
\frac{\partial \sigma}{\partial y}&=\epsilon^{-2}R^{-1}\left(\frac{\partial v}{\partial z}+\epsilon^2\left(-2\frac{\partial \eta}{\partial y}\frac{\partial v}{\partial y}-\frac{\partial \eta}{\partial x}\left(\frac{\partial v}{\partial x}+\frac{\partial u}{\partial y}\right)+\frac{\partial w}{\partial y}\right.\right.\\
&\quad\left.\left.-\frac{\partial \eta}{\partial y}^2\frac{\partial v}{\partial z}-\frac{\partial \eta}{\partial x}\frac{\partial \eta}{\partial y}\frac{\partial v}{\partial z}+2\frac{\partial \eta}{\partial y}\frac{\partial w}{\partial z}\right)+O(\epsilon^4)\right),\\
\frac{\partial \Gamma}{\partial t}+\frac{\partial(u\Gamma)}{\partial x}+\frac{\partial(v\Gamma)}{\partial y}&=\frac{c-\Gamma}{\tau^*}+O(\epsilon^2),\\
-\frac{K^*(c-\Gamma)}{\tau^*}&=\epsilon^{-2}Sc^{-1}R^{-1}\left(\frac{\partial c}{\partial z}+O(\epsilon^2)\right),\\
\sigma&=M_e^{-2}(1-\Gamma),
\end{aligned}\right\}\tag{3.3}$$

where all the quantities are evaluated at $z=1+\eta$, η being *a priori* of order unity. The non-dimensional adsorption–desorption time is represented by $\tau^*=\tau U/L$ and the virtual thickness of the interface by $K^*=K/H$. The elastic Mach number $M_e=U/v_e$ is the ratio of the flow velocity U to the elastic wave velocity v_e defined by (see Lucassen *et al.* 1970)

$$v_e=\sqrt{\frac{\sigma_r\Gamma_m}{\rho H}}.\tag{3.4}$$

3.2. *Asymptotic expansion*

We shall now proceed to an asymptotic expansion in ϵ. To do so we have to impose some constraints on the magnitude of the parameters (R, Sc, M, M_e, τ^*, K^*) in order to ensure the well posedness of the expansion while keeping as many physical phenomena as possible (see Bender & Orszag 1978). Of course, if one is interested in a particular limit, such as the two-dimensional incompressible or inviscid case, a much simpler analysis of equations (3.2), (3.3) may be carried out directly using more restrictive assumptions on the magnitude of the parameters. However, a general approach will be adopted here and particular limits will be derived from the master leading-order equations by letting parameters become large or small. One might wonder about the validity of such *a posteriori* changes in the magnitude of the parameters. In fact, the dynamics given by the master equations are identical to those that would have been

obtained directly provided the dominant term, at present the vertical viscous term, in the bulk equation is not modified. When a different magnitude of the Reynolds number will be considered a special comment on the validity of the expansion will be made. In all other cases the direct derivation is left to the curious readers.

Although the gauge functions (R, Sc, M) could be fixed using the dominant balance principle, we shall infer them from simple physical considerations. The crucial condition is that the transverse diffusion time scale H^2/ν should be small compared to the spanwise advection time scale L/U for the motion to be two-dimensional at leading order. This implies that $R\epsilon^2 \ll 1$ and corresponds to the usual lubrication approximation. We shall choose the gauge function $R = O(1)$ in order to keep the in-plane viscous effect of the same order as the inertia. The choice $R = O(\epsilon^{-1})$ will be mentioned in the last section and corresponds to the in-plane inviscid limit. Similarly, the condition that the soap concentration be at leading-order homogeneous across the film, imposes $ScR\epsilon^2 \ll 1$. We shall simply choose Sc of order unity even though actually Sc may be relatively large.

One must be careful about the pressure term in the z-momentum equation (3.2) since this term is large, $\epsilon^{-2}M^{-2} = M_b{}^{-2} = v_b^2/U^2$, and would be unbalanced without any further assumptions. Indeed, the bending wave velocity, which typically varies between 2 and 8 m s^{-1} in the experiments, is much larger than the mean velocity of the flow (10^{-2} to 1 m s^{-1}). The symmetry of the perturbation must be invoked to clarify this apparent paradox. If the perturbations of the two surfaces were antisymmetric (figure 3*a*), the pressure gradient normal to the film would be indeed the dominant term. This effect corresponds to the transfer (thanks to the pressure gradient in the z-direction) of the force resulting from the curvature of both surfaces of the membrane to the bulk fluid. The whole film, when antisymmetrically deformed (figure 3*a*), is then brought back to the horizontal position as if it were a solid membrane under a tension equal to twice the surface tension of the soap film. However, since only symmetric perturbations of the interfaces are considered in the present case, the pressure must be even in z implying that the leading-order transverse pressure gradient is zero (figure 3*b*). Only the in-plane pressure gradient may contribute in the leading-order dynamics. The scaling $M = O(1)$, equivalent to $M_b = M\epsilon$, realizes the balance with the inertia. Note that in Ida & Miksis (1998*a*) M_b is kept order unity. Under such circumstances, the leading-order dynamics correspond to the bending motion and the dynamics described here arise at the next order.

Finally, the non-dimensional adsorption–desorption time τ^* and the virtual thickness of the interface K^* will be assumed of order unity. This means that the chemical relaxation is allowed to act on the dynamical time scale L/U and that bulk fluid is a soap reservoir with, per unit surface of film, a number soap molecules diluted in the bulk fluid of the same magnitude as the number of soap molecules adsorbed on the surfaces. Fast adsorption–desorption processes will simply correspond to $\tau^* = 0$ and the surface soap concentration Γ will follow instantaneously the bulk concentration c evaluated at the interface. Equilibrium between the surface soap concentration and the bulk mean concentration will then be only limited by the diffusion of soap in the interstitial liquid as described by the last equation in the system (3.2).

Last but not least, the order of magnitude of the elastic Mach number M_e does not need to be specified since it appears in a single equation and may be considered as an independent expansion parameter.

Then, all the variables are expanded in series of ϵ^2 with the notation

$$f = f_0 + \epsilon^2 f_2 + \cdots. \tag{3.5}$$

3.2.1. *Leading-order equations*

The leading-order equations in the bulk fluid read

$$\left.\begin{aligned} \frac{\partial u_0}{\partial x}+\frac{\partial v_0}{\partial y}+\frac{\partial w_0}{\partial z}=0,\\ 0=R^{-1}\frac{\partial^2 u_0}{\partial z^2},\quad 0=R^{-1}\frac{\partial^2 v_0}{\partial z^2},\\ 0=-M^{-2}\frac{\partial p_0}{\partial z}+R^{-1}\frac{\partial^2 w_0}{\partial z^2},\\ 0=Sc^{-1}R^{-1}\frac{\partial^2 c_0}{\partial z^2}. \end{aligned}\right\} \tag{3.6}$$

Therefore, considering that u, v, and c are assumed even in z, then u_0, v_0 and c_0 are two-dimensional, i.e. are solely functions of (x, y). Consequently, since the symmetry imposes that w is odd in z

$$w_0=-(\nabla\cdot\boldsymbol{u}_0)z, \tag{3.7}$$

where $\nabla=(\partial/\partial x,\partial/\partial y)$ and $\boldsymbol{u}_0=(u_0,v_0)$ are the gradient and the leading-order velocity in the (x, y)-plane. The expression (3.7) for w_0 and the z-momentum equation in (3.6) imposes

$$0=-M^{-2}\frac{\partial p_0}{\partial z}, \tag{3.8}$$

i.e. the leading-order vertical pressure gradient is zero as anticipated from the symmetry consideration (figure 3*b*), implying that the leading-order pressure p_0 is only a function of (x, y) .

The boundary conditions at the upper surface involve quantities evaluated at $z=1+\eta_0$. Considering that, at the interface, $w_0=-(1+\eta_0)\nabla\cdot\boldsymbol{u}_0$ and $\partial w_0/\partial z=-\nabla\cdot\boldsymbol{u}_0$, the conditions read

$$\left.\begin{aligned} \frac{\partial\eta_0}{\partial t}+\boldsymbol{u}_0\cdot\nabla\eta_0=-(1+\eta_0)\nabla\cdot\boldsymbol{u}_0,\\ p_0+\left(\frac{\partial^2\eta_0}{\partial x^2}+\frac{\partial^2\eta_0}{\partial y^2}\right)=-2M^2R^{-1}\nabla\cdot\boldsymbol{u}_0,\\ 0=R^{-1}\frac{\partial u_0}{\partial z},\quad 0=R^{-1}\frac{\partial v_0}{\partial z},\\ \frac{\partial\Gamma_0}{\partial t}+\nabla\cdot(\Gamma_0\boldsymbol{u}_0)=\frac{c_0-\Gamma_0}{\tau^*},\\ 0=Sc^{-1}R^{-1}\frac{\partial c_0}{\partial z},\\ \sigma_0=M_e^{-2}(1-\Gamma_0). \end{aligned}\right\} \tag{3.9}$$

Three of the above equations are automatically fulfilled since (u_0, v_0, c_0) are independent of z. The remaining set of equations is not closed and should be completed by compatibility conditions coming from higher orders.

3.2.2. *Next order*

The compatibility conditions imposed by the second-order solution will give evolution equations for the leading-order free variables. To obtain them, it is only necessary to write the evolution equations involving three extra unknown second-order

fields (u_2, v_2, c_2):

$$\left.\begin{aligned}
\frac{\partial u_0}{\partial t} + \boldsymbol{u}_0 \cdot \nabla u_0 &= -M^{-2}\frac{\partial p_0}{\partial x} + R^{-1}\left(\frac{\partial^2 u_0}{\partial x^2} + \frac{\partial^2 u_0}{\partial y^2} + \frac{\partial^2 u_2}{\partial z^2}\right),\\
\frac{\partial v_0}{\partial t} + \boldsymbol{u}_0 \cdot \nabla v_0 &= -M^{-2}\frac{\partial p_0}{\partial y} + R^{-1}\left(\frac{\partial^2 v_0}{\partial x^2} + \frac{\partial^2 v_0}{\partial y^2} + \frac{\partial^2 v_2}{\partial z^2}\right),\\
\frac{\partial c_0}{\partial t} + \boldsymbol{u}_0 \cdot \nabla c_0 &= Sc^{-1}R^{-1}\left(\frac{\partial^2 c_0}{\partial x^2} + \frac{\partial^2 c_0}{\partial y^2} + \frac{\partial^2 c_2}{\partial z^2}\right),
\end{aligned}\right\} \tag{3.10}$$

and three boundary conditions at $z = 1+\eta_0$ (these equations do not involve η_2 terms):

$$\left.\begin{aligned}
\frac{\partial \sigma_0}{\partial x} &= R^{-1}\left(\frac{\partial u_2}{\partial z} - A_x\right),\\
\frac{\partial \sigma_0}{\partial y} &= R^{-1}\left(\frac{\partial v_2}{\partial z} - A_y\right),\\
-K^*\frac{c_0 - \Gamma_0}{\tau^*} &= Sc^{-1}R^{-1}\frac{\partial c_2}{\partial z},
\end{aligned}\right\} \tag{3.11}$$

where A_x and A_y are shear stresses at the interface coming from the zeroth-order solution:

$$\left.\begin{aligned}
A_x &= 2\frac{\partial \eta_0}{\partial x}\frac{\partial u_0}{\partial x} + \frac{\partial \eta_0}{\partial y}\left(\frac{\partial u_0}{\partial y} + \frac{\partial v_0}{\partial x}\right) + (1+\eta_0)\frac{\partial \nabla \cdot \boldsymbol{u}_0}{\partial x} + 2\frac{\partial \eta_0}{\partial x}\nabla \cdot \boldsymbol{u}_0,\\
A_y &= 2\frac{\partial \eta_0}{\partial y}\frac{\partial v_0}{\partial y} + \frac{\partial \eta_0}{\partial x}\left(\frac{\partial u_0}{\partial y} + \frac{\partial v_0}{\partial x}\right) + (1+\eta_0)\frac{\partial \nabla \cdot \boldsymbol{u}_0}{\partial y} + 2\frac{\partial \eta_0}{\partial y}\nabla \cdot \boldsymbol{u}_0.
\end{aligned}\right\} \tag{3.12}$$

Recalling that the symmetry imposes that (u, v, c) are even in z, equations (3.10) show that (u_2, v_2, c_2) are parabolic in z (Poiseuille like) since all the other terms involve the zeroth-order solution which does not vary with z. The boundary conditions (3.11) state that shear stresses associated with the vertical variations of (u_2, v_2) compensate zeroth-order shear stresses and surface tension gradient. Similarly, the second-order soap diffusive flux in the bulk fluid equilibrates the soap flux from the surface due to zeroth-order quantities. These boundary conditions (3.11) gives the expressions for (u_2, v_2, c_2):

$$\left.\begin{aligned}
u_2 &= \left(R\frac{\partial \sigma_0}{\partial x} + A_x\right)\frac{z^2}{2(1+\eta_0)} + U_2,\\
v_2 &= \left(R\frac{\partial \sigma_0}{\partial y} + A_y\right)\frac{z^2}{2(1+\eta_0)} + V_2,\\
c_2 &= Sc\,RK^*\frac{(c_0 - \Gamma_0)}{\tau^*}\frac{z^2}{2(1+\eta_0)} + C_2,
\end{aligned}\right\} \tag{3.13}$$

where (U_2, V_2, C_2) are functions of x and y only and do not need to be given explicitly further since we stop the expension at the present order. Elimination of u_2, v_2, c_2, p_0

and σ_0 in (3.10) gives, with (3.9), a complete set of leading-order equations:

$$\left.\begin{aligned} \frac{\partial \boldsymbol{u}_0}{\partial t} + \boldsymbol{u}_0 \cdot \nabla \boldsymbol{u}_0 &= \frac{-M_e^{-2}}{1+\eta_0}\nabla \Gamma_0 + M^{-2}\nabla\nabla^2\eta_0 + R^{-1}\nabla^2\boldsymbol{u}_0 + 3R^{-1}\nabla\nabla\cdot\boldsymbol{u}_0 + \frac{R^{-1}}{1+\eta_0}\boldsymbol{V}, \\ \frac{\partial \eta_0}{\partial t} + \nabla\cdot((1+\eta_0)\boldsymbol{u}_0) &= 0, \\ \frac{\partial c_0}{\partial t} + \boldsymbol{u}_0\cdot\nabla c_0 &= -\frac{K^*}{1+\eta_0}\frac{c_0-\Gamma_0}{\tau^*} + Sc^{-1}R^{-1}\nabla^2 c_0, \\ \frac{\partial \Gamma_0}{\partial t} + \nabla\cdot(\Gamma_0\boldsymbol{u}_0) &= \frac{c_0-\Gamma_0}{\tau^*}, \end{aligned}\right\} \tag{3.14}$$

where the vector $\boldsymbol{V} = (V_x, V_y)$ represents extra viscous terms given by

$$\left.\begin{aligned} V_x &= 2\frac{\partial \eta_0}{\partial x}\left(2\frac{\partial u_0}{\partial x} + \frac{\partial v_0}{\partial y}\right) + \frac{\partial \eta_0}{\partial y}\left(\frac{\partial u_0}{\partial y} + \frac{\partial v_0}{\partial x}\right), \\ V_y &= 2\frac{\partial \eta_0}{\partial y}\left(\frac{\partial u_0}{\partial x} + 2\frac{\partial v_0}{\partial y}\right) + \frac{\partial \eta_0}{\partial x}\left(\frac{\partial u_0}{\partial y} + \frac{\partial v_0}{\partial x}\right). \end{aligned}\right\} \tag{3.15}$$

In the limit of non-diffusing soap molecules, $Sc = \infty$, examined in the next section, the last two equations of (3.14) are replaced by

$$\left.\begin{aligned} \frac{\partial C_0}{\partial t} + \boldsymbol{u}_0\cdot\nabla C_0 &= 0, \\ \frac{\partial \Gamma_0}{\partial t} + \nabla\cdot(\Gamma_0\boldsymbol{u}_0) &= \frac{1}{\tau^*}\left(C_0 - \Gamma_0\left(1 + \frac{K^*}{1+\eta_0}\right)\right), \end{aligned}\right\} \tag{3.16}$$

where $C_0 \equiv c_0 + K^*\Gamma_0/(1+\eta_0)$ is the average volumic concentration of the soap that takes into account the soap contained in the bulk fluid and the surfaces. For the unperturbed film C_0 is equal to the mean value $C_m \equiv 1 + K^*$. The first equation simply expresses the local conservation of soap.

The system of equations (3.14) is fully equivalent to that obtained in § 3 of Ida & Miksis (1998*b*) if the Reynolds number R is set to unity and the adsorption–desorption time τ^* goes to infinity. The present study generalizes their results since an inertia-dominated evolution is accessible by setting $R = \infty$. Furthermore, the effect of soluble surfactant is included here. The study of Ida & Miksis (1998*b*) includes effects of the potential forces and of surface diffusivity that have been ignored here. In particular, van der Waals interaction forces are important for thin films and may be taken into account in the momentum equation (3.14) by adding the term

$$-\nabla W \tag{3.17}$$

where the attractive van der Waals potential is given by $W = A^*(1+\eta_0)^{-3}$ with $A^* = R^{-1}A_H/(H^2\rho v^2)$, A_H being the Hamaker constant (see Ida & Miksis 1998*b* for a discussion).

The system of equations (3.14) is very general since the first term on the right-hand side of the momentum equation accounts for the elasticity of the membrane, the second for the internal pressure gradient generated by the curvature of the surface (Young–Laplace law), the third for the viscous dissipation of the in-plane motion, the fourth and fifth terms for the viscous dissipation due to three-dimensional effects

(acting either through the pressure or through the shear stresses at the interface). The system (3.14) also takes into account the possibility of soluble soap (the insoluble limit corresponding to $\tau^* = \infty$) and variable bulk fluid soap concentration. The balance between these physical effects has been achieved by choosing an adequate gauge function for each parameter and each gives rise to terms in the set (3.14) that are weighted by the corresponding non-dimensional parameter.

In the next section, we show that the two-dimensional Navier–Stokes equations may only be recovered under specific limiting conditions. Indeed, the momentum equation in (3.14) closely resembles the two-dimensional Navier–Stokes equation with varying density, the surface soap density (through the surface tension σ_0 gradient) playing the role of the classical pressure while the thickness of the membrane $(1+\eta_0)$ is equivalent to a density. However it differs from the two-dimensional Navier–Stokes equation by the presence of curvature and viscous effects. Indeed three-dimensional pressure gradients introduce two extra effects coming from the curvature of the surface $-M^{-2}\nabla(\nabla^2\eta_0)$ and from the diagonal part of the shear stress tensor $2R^{-1}\nabla(\nabla\cdot\boldsymbol{u}_0)$. Similarly, viscous stresses tangent to the surface induce additional terms $R^{-1}\nabla(\nabla\cdot\boldsymbol{u}_0)$ and $R^{-1}\boldsymbol{V}/(1+\eta_0)$. The two terms $-M^{-2}\nabla(\nabla^2\eta_0)$ and $R^{-1}\boldsymbol{V}/(1+\eta_0)$ have no counterparts in the two-dimensional Navier–Stokes equation. On the other hand the term $4R^{-1}\nabla(\nabla\cdot\boldsymbol{u}_0)$ is familiar and may be reinterpreted as a dilatational viscosity. It is of the same order of magnitude as the two-dimensional viscous effect and always arises when averaging across a narrow dimension (see Ida & Miksis 1998*a* for references).

4. Particular limit flows

System (3.14) encompasses several different experimental situations if different limits of the parameters are considered. These limits may be obtained from the master system (3.14) by varying the order of magnitude of the non-dimensional parameters (R, Sc, M_b, M_e, τ^*, K^*).

4.1. *The incompressible limit*

The incompressible limit, certainly the most important for practical applications of soap tunnels, is obtained when the elastic Mach number M_e is small, i.e. when the typical velocity U is small compared to the Marangoni elastic wave velocity. These waves propagate at the speed $v_e = \sqrt{\sigma_r \Gamma_m/\rho H}$ as already given in equation (3.4). Taking the example of SDS soap molecules the waves travel at $4\,\mathrm{m\,s^{-1}}$ in a $10\,\mu\mathrm{m}$ thick film and at $13\,\mathrm{m\,s^{-1}}$ in a $1\,\mu\mathrm{m}$ thick film for a soap concentration of order 0.1% (see Couder *et al.* 1989 for details).

In the same way as for classical flows, small Mach number M_e implies that the relative variations of Γ_0 and therefore of η_0 are at most of order M_e^2. Variations of Γ_0 and η_0 which are equivalent to compressible effects are therefore weak for small elastic Mach number. These estimates are correct only if variations in bulk and surface soap concentrations are assumed to be small. Thickness variations due to compressibility and to bulk soap concentration become of the same order of magnitude if bulk soap concentration variations are of order M_e^2. This hypothesis excludes experiments where large thickness variations are initially present. This may be the case if vorticity is generated by moving a body through the film because of the presence of a meniscus that may detach from the body. Special care should be taken to avoid this artifact since then variations of thickness will be present in the leading-order momentum equation through the inertial term and the dynamics will be specific. Under these assumptions the system (3.14) simplifies considerably and follows at leading order the classical

Navier–Stokes equation. Of course this assumption might have been incorporated from the start of the derivation to obtain the leading-order incompressible dynamics, but then it would have been impossible to evaluate the discarded effects. Here we derive the same leading-order incompressible dynamics from the master system of equations (3.14) by making the assumption that M_e^2 is small.

Since $\delta \equiv M_e^2$ is an independent parameter we start a double expansion in δ with the chain rule:

$$f_0 = f_{00} + \mathrm{d} f_{01} + \mathrm{d}^2 f_{02} + \cdots. \tag{4.1}$$

For the moment, the parameter M will be assumed finite, but, as we are going to show, it will disappear from the leading-order dynamics. The parameter M should thus be rescaled if it should play a role in the dynamics. Therefore the present derivation would be valid even if M is smaller than one and a precise condition for the validity of the incompressible approximation is postponed to the end of the section.

4.1.1. *Order-1: the incompressibility condition*

The dominant term in the momentum equation in (3.14) is of order δ^{-1} and equals $(1+\eta_{00})^{-1}\nabla\Gamma_{00}$; therefore,

$$\Gamma_{00} = 1, \tag{4.2}$$

is the unique solution.

4.1.2. *Order 0: the Navier–Stokes equations*

Using (4.2), the equation for Γ_0 in (3.14) implies that the leading-order velocity is divergence free:

$$\nabla \cdot \boldsymbol{u}_{00} = 0, \tag{4.3}$$

with $\boldsymbol{u}_{00} = (u_{00}, v_{00})$. In turn, the transport equation of mass in (3.14) immediately implies that, if $\eta_{00} = 0$ initially (i.e. the initial deformations of the membrane are at most of order δ), it will remain so at all time:

$$\eta_{00}(x, y, t) = 0. \tag{4.4}$$

Since the surfaces of the film are flat at leading-order, the curvature and the viscous extra terms in the the momentum equation in (3.14) become of order δ. Therefore, the dominant viscous dissipation occurs as a two-dimensional flow and the leading-order momentum equation simplifies in:

$$\frac{\partial \boldsymbol{u}_{00}}{\partial t} + \boldsymbol{u}_{00} \cdot \nabla \boldsymbol{u}_{00} = -\nabla\Gamma_{01} + R^{-1}\nabla^2 \boldsymbol{u}_{00}. \tag{4.5}$$

The system (4.3, 4.5) corresponds to the incompressible two-dimensional Navier–Stokes equations for the zero-order velocity $\boldsymbol{u}_{00}$ where Γ_{01} is a first-order term, which plays the role of pressure, and obeys the Poisson equation:

$$\nabla^2\Gamma_{01} = -\nabla \cdot (\boldsymbol{u}_{00} \cdot \nabla \boldsymbol{u}_{00}). \tag{4.6}$$

When boundary conditions for Γ_{01} are specified on a contour or at infinity, Γ_{01} is uniquely determined by (4.6).

It is quite remarkable that $M_e \ll 1$, i.e. $U \ll v_e$, is a sufficient condition for the soap film to be ruled by the usual incompressible two-dimensional Navier–Stokes equations. Now that the derivation has been carried out, one may notice that the curvature term will enter the leading-order dynamics if $M^{-2}M_e^2$ and M_e^{-2} are of the same order. This is because the order of the curvature term is overestimated when

M^{-2} and M_e^{-2} are small since the membrane is not deformed at leading order (since η_0 is order M_e^{-2} when M_e is small). Therefore the weakest constraints under which (4.6) describes the leading-order dynamics is that M_e should be small and M should be such that $M_e^{-2} \gg M^{-2}M_e^2$ for the curvature effect to be really negligible. This imposes, recalling that $M = M_b L/H$, that $U \ll v_e^2 L/Hv_b$. This condition is in practice always verified: the small elastic Mach number assumption imposes $U \ll v_e$ and $v_e \ll v_e(v_e L/Hv_b)$ since v_b and v_e are, usually in experiments, of the same order and L/H is extremely large. This result is good news for the validity of experiments since often v_b is smaller than v_e and U/v_b is larger than unity.

4.1.3. *Order-1: a decoupled equation for the thickness variations*

In his pioneering experiments, Couder (1981) observed that the thickness variations provided an excellent visualization of the film motion. When the film is lit by a white spot, rainbow iridescence appears on the surface, the colours varying with the local thickness of the membrane. When a monochromatic lamp (a yellow low-pressure sodium lamp usually used for street and parking lot lighting) is used, bright fringes mark the film wherever its thickness is an odd multiple of quarter-wavelength. Gharib & Derango (1989) used the white light technique in their soap film experiments and so did Wu *et al.* (1995), Afenchenko *et al.* (1998) and others. In all those studies, many details were revealed by visualization such as filaments between vortices, pairing of vortices, and fine-scale structures inside vortex cores. A purely elastic model of the soap film that will intuitively link thickness variations to the variation of pressure cannot explain the appearance of such small flow structures. New experiments by Rivera *et al.* (1998) and Vorobieff *et al.* (1999) have shown that the thickness field behaves both as a passive scalar and as a visualization of the vorticity. Such behaviour has been already anticipated by Chomaz & Cathalau (1990) and Chomaz & Costa (1998) where dynamical equations for the in-plane velocity, film thickness, and soap concentrations were guessed using the idea of *soap film particle* and integrated conservation of mass, momentum and soap. Compared to the present asymptotic theory their heuristic approach turns out to give the correct dynamics except for the dissipative and for the curvature term. Therefore the thickness dynamics at small elastic Mach number they have analysed are also correct. The analysis identifies precisely different contributions to the thickness variations that seem to explain even the more recent experimental observations. In particular they show that the chemical relaxation may explain why the thickness correlates to the vorticity field. This section will follow the same spirit as these early studies. The expansion will be carried out to the next order to get an evolution equation for the thickness variations η_{01} since they are small and are not accounted for in the leading-order dynamics.

For simplicity only the case with non-diffusive soap, $Sc = \infty$, will be considered and equations (3.16) will be used. To be compatible with (4.4) we set $C_{00} = 1 + K^*$. This correspond to the hypothesis that initial variations of total soap concentration are small. If this were not the case, the initial thickness variations would not have been small and η_{00} would not have been zero. The useful first-order equations read

$$\left.\begin{aligned} \frac{\partial \eta_{01}}{\partial t} + \boldsymbol{u}_{00}\cdot\nabla\eta_{01} + \nabla\cdot\boldsymbol{u}_{01} &= 0, \\ \frac{\partial C_{01}}{\partial t} + \boldsymbol{u}_{00}\cdot\nabla C_{01} &= 0, \\ \frac{\partial \Gamma_{01}}{\partial t} + \boldsymbol{u}_{00}\cdot\nabla\Gamma_{01} + \nabla\cdot\boldsymbol{u}_{01} &= \frac{C_{01} + K^*\eta_{01} - \Gamma_{01}(1+K^*)}{\tau^*}, \end{aligned}\right\} \tag{4.7}$$

with $\boldsymbol{u}_{01} = (u_{01}, v_{01})$. The first-order velocity, $\boldsymbol{u}_{01}$, is eliminated by subtracting the first and third equations. The resulting evolution equation applies on the field $(\eta_{01} - \Gamma_{01})$. As a result, we introduce the new field h_1 representing the thickness variations departing from the Marangoni equilibrium. More precisely h_1 is defined by

$$h_1 = K^*(\eta_{01} - \Gamma_{01}) + C_{01}, \tag{4.8}$$

where the effect of the variations of total soap concentration C_{01} has been taken into account. With this definition, h_1 obeys the relaxation equation:

$$\frac{\partial h_1}{\partial t} + \boldsymbol{u}_{00} \cdot \nabla h_1 = \frac{h_1 - \Gamma_{01}}{\tau'}, \tag{4.9}$$

with $\tau' = \tau^*/K^*$.

This equation is closed since Γ_{01} was determined at the previous order and is given by (4.6). According to equation (4.8), three terms contribute to the thickness variations: $\eta_{01} = \Gamma_{01} - C_{01}/K^* + h_1/K^*$. The two last contributions are weighted by $1/K^*$ so that they may be extremely large for thick films ($K \ll H$). The physical meaning of these three terms is the following:

(i) the surface concentration of soap Γ_{01}, computed in (4.6), accounts for the Marangoni elasticity of the film. It plays the role of the pressure and induces thickness variations in the same way as pressure variations generate density variations in an isothermal gas.

(ii) the total concentration of soap C_{01} is simply advected as a passive scalar (second equation of (4.7)). However, variations of soap concentration play a key role through the state laws (equations (2.12), (2.11)) linking locally the surface tension to the surface soap concentration: the higher C_{01} the thinner the film for a given surface tension. This term induces thickness variations in the same manner as the temperature variations induce density variations in a classical gas.

(iii) the additional field h_1 has no equivalent in gas. The chemical kinetics for the adsorption–desorption of soap forces the thickness to follow the *pressure* perturbation on a time scale τ'. The evolution of the field h_1 is not trivial. If we set $C_{01} = 0$ for clarity then three cases can be considered that throw light on the dynamics of h_1:

– for small τ' equation (4.9) imposes that $h_1 = \Gamma_{01}$ at all times, and therefore equation (4.8) gives

$$\eta_{01} = \Gamma_{01} + h_1/K^* = \frac{1 + K^*}{K^*}\Gamma_{01}, \tag{4.10}$$

the Gibbs response of the thickness to a variation of *pressure* Γ_{01};

– for large τ', the right-hand side of equation (4.9) is close to zero implying $h_1 = 0$ at all times if $h_1 = 0$ initially. Thus, η_{01} follows a Marangoni type variation:

$$\eta_{01} = \Gamma_{01}; \tag{4.11}$$

– for τ' of order unity, the field h_1 should be computed via numerical simulation for each particular flow. Results obtained by Chomaz & Costa (1998) on the evolution of the field h_1 governed by the same equation (4.8) are reported in table 1. In their simulations the field h_1 is initially set to zero and the computed velocity field corresponds to the nonlinear evolution of a wake profile, in a very large computational box, initially subjected to random perturbations (see Chomaz & Costa 1998 for details). The numerical simulation shows, as reported on table 1, that for τ' of order unity the amplitude of h_1 is large and the field h_1 is well correlated to the enstrophy field ω^2. The correlation is even higher if only the zones where the enstrophy is larger than 5% of the enstrophy maximum are considered. We see from table 1 that the

τ'	0.2	2	10	20	100	1000
Correlation with ω^2	0.65	0.90	0.95	0.94	0.94	0.93
Correlation with ω^2 with a 5% threshold	0.70	0.93	0.98	0.98	0.98	0.98
Maximum amplitude of h_1	0.29	0.26	0.14	0.083	0.02	0.002
Same rescaled by the maximum amplitude of Γ_{01}	1.	0.9	0.5	0.3	0.07	0.007

TABLE 1. A summary of the results from the prototype experiment by Chomaz & Costa (1998). The correlation coefficient between h_1 and ω^2 and the maximum amplitude of h_1 have been computed at time $t = 16$, the wake velocity defect and the Bickley wake width being both unity. At time $t = 16$, pairing events are already taking place in the numerical simulation. The field h_1 was initially zero since prior to the start of the experiment the film was at equilibrium. The maximum amplitude of h_1 is compared to 0.29, the maximum amplitude of the pressure contribution Γ_{01}.

correlation between h_1 and ω^2 increases with τ' and is already equal to 93% for $\tau' = 2$. The corresponding amplitude of h_1 equals 0.26 and decreases with increasing τ'.

The value of τ' is therefore crucial to evaluate the variations of thickness due to the chemical relaxation. This effect may explain the correlation between the soap film thickness and the vorticity observed in experiments and measured by Vorobieff *et al.* (1999). From the present analysis, we see that, since the contribution to the thickness variations of the relaxing field h_1 is weighted by $1/K^*$ in equation (4.8), it will be dominant when K^* is small. The smallness of K^* means that the reservoir effect of the interstitial fluid is large. This will be the case for highly soluble surfactant and relatively thick films for which the amount of soap adsorbed on the surface is small compared to the amount in solution in the bulk fluid. For SDS soap molecules in a 10 μm thick film, $1/K^*$ is approximately 3 and if τ' is assumed about unity, the relaxing field h_1 will account for 70% of the total thickness variations.

In Vorobieff *et al.*'s (1999) experiment, the thickness of the film was not uniform even at the first instants of the experiment, i.e. close to the grid that was generating the turbulence. These initial variations of thickness are accounted for through the instantaneous elasticity of the film (the Marangoni elasticity corresponding to the Γ_{01} term in equation (4.8)). Vorobieff *et al.* (1999) invoke the shedding of vortices with non-uniform thickness due to a meniscus effect. In the present framework, this effect would be modelled by an initial variation in the total soap concentration C_{01}. This contribution, governed by the second equation of (4.7), evolves as a passive scalar in qualitative agreement with their observations. Since Vorobieff *et al.* are able to measure experimentally both the velocity field and the thickness variations they may eventually test the validity of (4.8) using a numerical simulation to compute both the C_{01} and the h_1 contributions and their weight compared to the pressure effect Γ_{01}.

4.2. *The inviscid limit and supersonic soap film*

Since some soap film experiments are carried out with a soap Mach number M_e of order unity, one should determine whether or not the flow obeys compressible two-dimensional Navier–Stokes equations. By inspection of (3.14), it is clear that this will never be the case if viscous effect are important. Therefore the only hope of using soap films to perform two-dimensional compressible hydrodynamics experiments is when the Reynolds number is large $R \gg 1$. This assumption seems *a priori* contradictory to

the expansion procedure we used, since it is based on the dominance of the transverse viscous term. In fact, this is not the case if the transverse diffusion time scale is kept smaller than the in-plane advection time U/L. This corresponds to the condition $Re \ll \epsilon^{-2}$ ($\epsilon = H/L$) which ensures that the leading-order flow is two-dimensional. Large Reynolds number flow would be achieved by assuming, in the expansion procedure, $Re = \epsilon^{-1}\mathscr{R}$. In that case the internal Poiseuille flow, that transfers the surface forces, due to the surface tension gradient, to the bulk fluid, would be of order ϵ (instead of order ϵ^2). As a result all the viscous terms, including the usual two-dimensional dissipation, would disappear from the leading-order dynamics. We obtain the same equation if Re is *a posteriori* assumed of order ϵ^{-1} in the equations (3.14). In that case, using the simplified equations (3.16), the system (3.14) becomes

$$\left.\begin{aligned} \frac{\partial \boldsymbol{u}_0}{\partial t} + \boldsymbol{u}_0 \cdot \nabla \boldsymbol{u}_0 &= \frac{-M_e^{-2}}{1+\eta_0}\nabla \Gamma_0 + M^{-2}\nabla\nabla^2\eta_0 \\ \frac{\partial \eta_0}{\partial t} + \nabla \cdot (1+\eta_0)\boldsymbol{u}_0 &= 0, \\ \frac{\partial C_0}{\partial t} + \boldsymbol{u}_0 \cdot \nabla C_0 &= 0, \\ \frac{\partial \Gamma_0}{\partial t} + \nabla \cdot (\Gamma_0 \boldsymbol{u}_0) &= \frac{1}{\tau^*}\left(C_0 - \Gamma_0\left(1 + \frac{K^*}{1+\eta_0}\right)\right), \end{aligned}\right\} \tag{4.12}$$

The third equation of (4.12) expresses the local conservation of the total soap concentration; if we assume that C_0 were uniform initially it will remain so and for all time we will have $C_0 = 1 + K^*$.

The curvature term $M^{-2}\nabla\nabla^2\eta_0$ in the momentum equation is usually negligible in the experiments since the elastic waves and the bending wave propagate at about the same speed ($v_e \sim v_b$). Therefore $M_e \sim M_b$ and the M^{-2} term in (4.12) is negligible as $M = M_b\epsilon^{-1} \sim M_e\epsilon^{-1} \gg M_e$.

However, the inviscid dynamics described by (4.12) are very specific to a soap film if τ^* is of order one, i.e. if the chemical adsorption–desorption time is of the same order as the dynamical time L/U. Fortunately, in many practical applications, these 'supersonic' flows involve rapid motion and, therefore, the surfactant can be assumed insoluble (i.e. $\tau^* = \infty$).

Then under the three extra assumptions that C_0 is initially uniform, M_e and M_b are of the same order, and τ^* is large, the equations (4.12) take the familiar form

$$\left.\begin{aligned} \frac{\partial \boldsymbol{u}_0}{\partial t} + \boldsymbol{u}_0 \cdot \nabla \boldsymbol{u}_0 &= \frac{-M_e^{-2}}{1+\eta_0}\nabla \Gamma_0 \\ \frac{\partial \eta_0}{\partial t} + \nabla \cdot (1+\eta_0)\boldsymbol{u}_0 &= 0, \\ \frac{\partial (\Gamma_0/(1+\eta_0))}{\partial t} + \boldsymbol{u}_0 \cdot \nabla \frac{\Gamma_0}{1+\eta_0} &= 0. \end{aligned}\right\} \tag{4.13}$$

The last equation stipulates that $\Gamma_0/(1+\eta_0)$ is a constant of the motion in the same manner as p/ρ in an isothermal gas. However, in usual compressible flows, the dynamics are not isothermal but isentropic so that the quantity conserved with the motion is actually p/ρ^γ with γ the rato of specific heat capacities. Therefore, compressible soap flows are still unusual since the constant γ should be set to the value 1 which is not physical for usual gases.

5. Conclusion

Under the assumption that the motion in the plane of the film occurs on a large scale compared to the thickness of the film, a very general system of equations describing soap film dynamics has been derived. This *master* model takes into account a large number of physical effects: film elasticity, film stiffness (curvature effect), viscosity, diffusion, arbitrary large variations of thickness, adsorption and desorption of the soap (solubility of the soap) and non-uniform initial soap concentration. It extends the work of Ida & Miksis (1998*a*, *b*) to arbitrary inertial effects and to a soluble surfactant. Following Ida & Miksis (1998*a*, *b*), De Wit *et al.* (1994), Erneux & Davis (1993), Edwards & Oron (1995), and Oron *et al.* (1997) many other effects, ignored here for the sake of clarity, such as van der Waals forces, gravity forces, surface viscosity, surface diffusivity, or evaporation may be incorporated directly in the model when suggested by experimental evidence. Except when soap films are flowing in vacuum, air friction should be taken into account. It can be physically modelled as discussed in Couder *et al.* (1989) by a Rayleigh damping term proportional to velocity. Recent experiments by Rivera & Wu (2000) have confirmed the validity of this model.

The major novelty of the present study is the systematic analysis of the dynamics encompassed in the master model by considering limit values for the non-dimensional parameters. The equations describing leading-order soap films are two-dimensional but do not correspond to any classical two-dimensional dynamics except in two limit cases:

(i) If the elastic Mach number M_e is small, i.e. if the flow velocity is smaller than the Marangoni elastic wave speed and if the initial non-uniformities of the film thickness and total soap concentration are small, then the soap film does obey the incompressible Navier–Stokes equations. This is not the case if initial thickness variations are large. In particular when the motion is generated by a moving transverse boundary, one has to avoid the detachment of the meniscus. Therefore the present theory legitimates the use of soap films for turbulence studies. In that case, despite the fact that the leading-order flow in the film is decoupled from the thickness variations, we have shown that the thickness variations are linked to the motion of the film in a non-trivial manner. Three different contributions to the thickness variations have been identified, with weight depending on K^*, the ratio between the amount of soap adsorbed on the surface and in solution in the bulk fluid. The instantaneous Marangoni elasticity induces thickness variations proportional to the two-dimensional pressure field. The long-time Gibbs elasticity, due to soap molecules migrating between the surface and the bulk fluid, produces thickness variations correlated to the vorticity field as demonstrated by numerical simulations. The initial thickness variations associated with initial inhomogeneities in total soap concentrations produces thickness variations that evolve as if the thickness were a passive scalar. In a particular experiment, one of these three effects may dominate depending on the mean thickness of the film, the solubility and mobility of the soap used, and the initial inhomogeneities in thickness produced by the specific device that creates the soap film flow.

(ii) If the elastic Mach number M_e is order one, the Reynolds number is large, and the solubility of the soap is neglected, then soap films obey at leading order the compressible Euler equation but for a two-dimensional gas with an unusual $\gamma = 1$ constant.

In all the other cases the dynamics are specific to soap films since physical effects, that have no equivalent in classical fluids, enter the leading-order dynamics described by the master equation (3.14).

In all published works using soap films to model two-dimensional flows, the parameter values involved in the present analysis are unknown. In particular elasticity is strongly dependent on the experimental device that creates the film and the adsorption–desorption time is known to vary dramatically according to the presence of minor chemical species (pollutants). The physical parameters appearing in the master equation set might be retrieved by conducting simple wave propagation experiments. Indeed, the master system predicts that elastic waves should obey the dispersion relation:

$$i\omega(\omega^2 - k^2 v_e^2) - \frac{1+K^*}{\tau}\left(\omega^2 - k^2 v_e^{-2}\frac{K^*}{1+K^*}\right) = 0, \tag{5.1}$$

where k is the modulus of the dimensional wave vector $\boldsymbol{k}$, and ω the dimensional frequency. Measuring in experiments the phase speed of the elastic waves as a function of the frequency should give access to v_e, K^*, and τ. When $\omega \gg \tau^{-1}$, the soap is insoluble and (5.1) describes the Marangoni elastic waves. These waves are non-dispersive and propagate at the speed $v_e = \sqrt{\sigma_r \Gamma_m/\rho H}$ as already given in equation (3.4). Taking the example of SDS soap molecules, the waves travel at $4\,\mathrm{m\,s^{-1}}$ in a $10\,\mu\mathrm{m}$ thick film and at $13\,\mathrm{m\,s^{-1}}$ in a $1\,\mu\mathrm{m}$ thick film for a soap concentration of order 0.1%. The limit $\omega \ll \tau^{-1}$ corresponds to an instantaneous equilibrium between the bulk film and the soap. The elastic waves then propagate at the speed $v_G = v_e\sqrt{K^*/(1+K^*)}$.

Using the present analysis, such measurements should enable all the possible artifacts associated with the use of a soap film to be precisely quantified. This would be crucial for the interpretation of soap film experimental results. If the elastic Mach number is really small then such a determination should allow a precise analysis of the thickness variation measurements. But, in many experiments, the velocities used are not so small and the elastic Mach number is very often of the order 0.3 or larger. In that case, once the elasticity and adsorption–desorption time are measured, the present theory should give precise estimates of the neglected effects. In particular for two-dimensional turbulence experiments it should define a lower bound for the vorticity cascade, below which neither three-dimensional dissipation nor curvature effects can be neglected. Similarly it should predict an upper bound to the inverse energy cascade beyond which compressibility and relaxation due to adsorption–desorption can no longer be ignored. As already discussed, air friction should also be taken into account to make this upper bound more precise.

P. Billant, F. Gallaire, and R. Lingwood are kindly acknowledged for their support and the careful and patient reading of the manuscript. Y. Couder is greatly acknowledged for giving me a role in the first episode of the Soap Film Opera back in the eigthies. W. S. has inspired the present theoretical work since two-dimensional or not two-dimensional?: that is the question I have tried to answer, despite the slings and arrows of asymptotic expansion, to secure the fortune of soap film experiments, and that was the original title of the present article.

REFERENCES

Afenchenko, V. O., Ezersky, A. B., Kiyashko, S. V., Rabinovich, M. I. & Weidman, P. D. 1998 The generation of two-dimensional vortices by transverse oscillation of a soap film. *Phys. Fluids* **10**, 390–399.

Bender, C. M. & Orszag, S. A. 1978 *Advanced Mathematical Methods for Scientists and Engineers.* McGraw-Hill.

Boudaoud, A., Couder, Y. & Ben Amar, M. 1999 Self-adaptation in vibrating soap films. *Phys. Rev. Lett.* **82**, 3847–3850.

Boys, C. V. 1890 *Soap Bubbles and the Forces which Mould them.* Society for promoting Christian knowledge, London and Anchor books, New York.

Burgess, J. M., Bizon, C., McCormick, W. D., Swift, J. B. & Swinney, H. L. 1999 Instability of the Kolmogorov flow in a soap film. *Phys. Rev.* E **60**, 715–721.

Chomaz, J.-M. & Cathalau, B. 1990 Soap films as two-dimensional classical fluids. *Phys. Rev.* A **41**, 2243–2246.

Chomaz, J.-M. & Costa, M. 1998 Thin films dynamics. In *Free Surface Flows* (ed. H. C. Kuhlmann & H.-J. Rath), pp. 44–99, CISM Courses & Lectures No. 391, Springer.

Couder, Y. 1981 The observation of a shear flow instability in a rotating system with a soap membrane. *J. Phys. Lett.* **42**, 429–431.

Couder, Y., Chomaz, J. M. & Rabaud, M. 1989 On the hydrodynamics of soap films. *Physica* D **37**, 384–405.

De Wit, A., Gallez, D. & Christov, C. I. 1994 Nonlinear evolution equations for thin liquid films with insoluble surfactants. *Phys. Fluids* **6**, 3256–3266.

Edwards, D. A. & Oron, A. 1995 Instability of a non-wetting film with interfacial viscous stress. *J. Fluid Mech.* **298**, 287–309.

Erneux, T. & Davis, S. H. 1993 Nonlinear rupture of free films. *Phys. Fluids* A **5**, 1117–1122.

Fauve, S. 1988 Waves on interfaces. In *Free Surface Flows* (ed. H. C. Kuhlmann & H.-J. Rath), pp. 44–99, CISM Courses & Lectures No. 391, Springer.

Fliert, B. W. van de, Howell, P. D. & Ockendon, J. R. 1995 Pressure-driven flow of a thin viscous sheet. *J. Fluid Mech.* **292**, 359–376.

Gharib, M. & Derango, P. 1989 A liquid film tunnel to study two-dimensional flows. *Physica* D **37**, 406–416.

Goldburg, W. I., Rutgers, M. A. & Wu, X. L. 1997 Experiments on turbulence in soap films. *Physica* A **239**, 340–346.

Gibbs, J. W. 1931 *The Collected Works.* Longmans Green.

Horváth, V. K., Cressman, J. R., Goldburg, W. I. & Wu X. L. 2000 Hysteresis at low Reynolds number: Onset of two-dimensional vortex shedding. *Phys. Rev.* E **65**, 4702–4705.

Ida, M. P. & Miksis, M. J. 1995 Dynamics of a lamella in a capillary tube. *SIAM J. Appl. Maths* **55**, 23–57.

Ida, M. P. & Miksis, M. J. 1998*a* Dynamics of thin films I: general theory. *SIAM J. Appl. Maths* **58**, 456–473.

Ida, M. P. & Miksis, M. J. 1998*b* Dynamics of thin films II: applications. *SIAM J. Appl. Maths* **58**, 474–500.

Kellay, H., Wu, X. L. & Goldburg, W. 1995 Experiments with turbulent soap films. *Phys. Rev. Lett.* **74**, 3875–3878.

Kellay, H., Wu, X. L. & Goldburg, W. 1998 Vorticity measurements in turbulent soap films. *Phys. Rev. Lett.* **80**, 277–280.

Levich, V. G. & Krylov, V. S. 1969 Surface-tension-driven phenomena. *Ann. Rev. Fluid Mech.* **1**, 293–316.

Lucassen, J., Van Den Tempel, M., Vrij, A. & Hesselink, F. 1970 *Proc. K. Ned. Akad. Wetensch. B* **73**, 109–124.

Martin, B. K., Wu, X. L., Goldburg, W. I. & Rutgers, M. A. 1998 Spectra of decaying turbulence in soap films. *Phys. Rev. Lett.* **80**, 3964–3967.

Mysels, K. J., Shinoda, K. & Frankel, S. 1959 *Soap Films, Studies of their Thinning.* Pergamon.

Oron, A., Davis, S. H. & Bankoff, S. G. 1997 Long-scale evolution of thin liquid film. *Rev. Mod. Phys.* **69**, 931–980.

Paret, J. & Tabeling, P. 1997 Experimental observation of the two-dimensional inverse energy cascade. *Phys. Rev. Lett.* **79**, 4162–4165.

Plateau, J. 1870 *Statique Expérimentale et Théorique des Liquides Soumis aux Seules Forces Moléculaires.* Gauthier Villars.

Prévost, M. & Gallez, D. 1986 Nonlinear rupture of thin free liquid films. *J. Chem. Phys.* **84**, 4043–4048.

Rivera, M., Vorobieff, P. & Ecke, R. E. 1998 Turbulence in flowing soap films: velocity, vorticity and thickness fields. *Phys. Rev. Lett*. **81**, 1417–1480.

Rivera, M. & Wu, X. L. 2000 External dissipation in driven two-dimensional turbulence. *Phys. Rev. Lett*. **85**, 976–979.

Rusanov, A. L. & Krotov, V. V. 1979 Gibbs elasticity of liquid films. *Prog. Surf. Memb. Sci*. **13**, 415–524.

Rutgers, M. A., Wu, X. L. & Bhagavatula, R. 1996 Two-dimensional velocity profiles and laminar boundary layers in flowing soap films. *Phys. Fluids* **8**, 2847–2854.

Savart, F. 1833*a* Mémoire sur le choc d'une veine liquide lancée contre un plan circulaire. *Ann. Chim. Phys*. **54**, 55–87.

Savart, F. 1833*b* Mémoire sur le choc de deux veines liquides animées de mouvements directement opposés. *Ann. Chim. Phys*. **54**, 257–310.

Sharma, A. & Ruchenstein, E. 1986 Rupture of thin free films with insoluble surfactants: Non-linear aspects. *AIChE Symp. Ser*. **252**, 129–144.

Squire, H. B. 1953 Investigation of the stability of a moving liquid film. *Ann. Chim. Phys*. **54**, 257–310.

Stone, H. A. 1990 A simple derivation of the time-dependent convective-diffusion equation for surfactant transport along a deforming interface. *Phys. Fluids* A **2**, 111–112 .

Taylor, G. I. 1959 The dynamics of thin sheets of fluid, II – waves on fluid sheets. *Proc. R. Soc. Lond*. A **253**, 296–312.

Vega, J. M., Higuera, F. J. & Weidman, P. D. 1998 Quasi-steady vortical structures in vertically vibrating soap films. *J. Fluid Mech*. **372**, 213–230.

Vorobieff, P., Rivera, M. & Ecke, R. E. 1999 Soap film flows: Statistics of two-dimensional turbulence. *Phys. Fluids* **11**, 2167–2177.

Waxman, A. M. 1984 Dynamics of a couple-stress fluid membrane. *Stud. Appl. Maths* **70**, 63–86.

Wu, X., Martin, B. K., Kellay, H. & Goldburg, W. 1995 Hydrodynamic convection in a two-dimensional Couette cell. *Phys. Rev. Lett*. **75**, 236–239.